Functional and Morphologic Alterations in Mechanical, Polymodal, and Cold Sensory Nerve Fibers of the Cornea Following Photorefractive Keratectomy

Federico Bech,[1] Omar González-González,[1] Enol Artime,[1] Joana Serrano,[1] Ignacio Alcalde,[1] Juana Gallar,[2] Jesús Merayo-Lloves,[1] and Carlos Belmonte[1,2]

[1]Instituto Universitario Fernández-Vega, Universidad de Oviedo & Fundación de Investigación Oftalmológica, Oviedo, Spain
[2]Instituto de Neurociencias, Universidad Miguel Hernández-CSIC, San Juan de Alicante, Spain

Correspondence: Carlos Belmonte, Instituto de Neurociencias, UMH-CSIC, Avenida Santiago Ramón y Cajal, San Juan de Alicante, 203550, Spain;
carlos.belmonte@umh.es.

FB and OG-G contributed equally to the work presented here and should therefore be regarded as equivalent authors.

Submitted: February 5, 2018
Accepted: April 4, 2018

Citation: Bech F, González-González O, Artime E, et al. Functional and morphologic alterations in mechanical, polymodal, and cold sensory nerve fibers of the cornea following photorefractive keratectomy. *Invest Ophthalmol Vis Sci*. 2018;59:2281–2292. https://doi.org/10.1167/iovs.18-24007

Purpose. To define the characteristics and time course of the morphologic and functional changes experienced by corneal sensory nerves after photorefractive keratectomy (PRK).

Methods. Unilateral corneal excimer laser photoablation was performed in 54 anesthetized 3- to 6-month-old mice; 11 naïve animals served as control. Mice were killed 0, 3, 7, 15, and 30 days after PRK. Excised eyes were placed in a recording chamber superfused at 34°C. Electrical nerve impulse activity of single sensory terminals was recorded with a micropipette applied onto the corneal surface. Spontaneous and stimulus-evoked (cold, heat, mechanical, and chemical stimuli) nerve terminal impulse (NTI) activity was analyzed. Corneas were fixed and stained with anti–β-Tubulin III antibody to measure nerve density and number of epithelial nerve penetration points of regenerating subbasal leashes.

Results. Nerve fibers and NTI activity were absent in the injured area between 0 and 7 days after PRK, when sparse regenerating nerve sprouts appear. On day 15, subbasal nerve density reached half the control value and abnormally responding cold-sensitive terminals were recorded inside the lesion. Thirty days after PRK, nerve density was almost restored, active cold thermoreceptors were abundant, and polymodal nociceptor activity first reappeared.

Conclusions. Morphologic regeneration of subbasal corneal nerves started shortly after PRK ablation and was substantially completed 30 days later. Functional recovery appears faster in cold terminals than polymodal terminals, possibly reflecting an incomplete damage of the more extensively branched cold-sensitive axon terminals. Evolution of postsurgical discomfort sensations quality may be associated with the variable regeneration pattern of each fiber type.

Keywords: nerve regeneration, photorefractive keratectomy, cold thermoreceptors, polymodal nociceptors, dysesthesia

Photorefractive surgery (PRK) is usually accompanied by decreased corneal sensitivity, transitory tear deficiency, and symptoms of dry eye.[1–4] These disturbances are due in a large extent to damage of corneal sensory nerves. Peripheral nerve injury alters sensory input to the somatosensory cortex and to brainstem centers responsible for corneal sensation, blinking, and reflex parasympathetic stimulation of lacrimal gland secretion.[5,6] This results in dysesthesias, reduced blinking rate, and decreased basal production of the aqueous component of the tear film.[7–10]

During the first 24 hours after PRK, a local inflammatory reaction develops in the injured cornea.[11] Macrophages, monocytes, T cells, and polymorphonuclear cells infiltrate and remove damaged epithelium debris.[12] Release of cytokines, chemokines, and growth factors by injured epithelial cells and keratocytes of the anterior stroma, and by resident and migrating inflammatory cells, rapidly activates repair processes including migration and mitosis of healthy epithelial cells, nerve regrowth, and stromal healing.[13,14] Regeneration of corneal nerves after PRK occurs as a biphasic process. First, branches of the subepithelial nerve plexus at the margin of the injury site reconstruct a transient subbasal plexus composed by fine neurites that run centrally with migrating cells. In a second stage, this plexus degenerates and is replaced by nerves originating from the underlying stroma.[15,16] However, the recovery of subbasal nerve density is gradual and not complete until 2 to 3 years after surgery.[17,18]

Trigeminal ganglion sensory neurons innervating the cornea are functionally heterogeneous and have been classified as polymodal nociceptor, mechano-nociceptor, and cold thermoreceptor neurons, on the basis of intensity and form of energy (mechanical, thermal, chemical) that activates preferentially their peripheral corneal terminals.[19,20] Each functional class of corneal neuron evokes qualitatively distinct conscious sensations[21,22] and contributes differently to the modulation of tearing and blinking.[20,23,24] Experimental evidence suggests that mechano-nociceptors are important in evoking acute pricking pain when the cornea is mechanically stimulated, while activation of polymodal nociceptors by mechanical, thermal, or chemical noxious stimuli evokes burning pain, hyperalgesia, and neurogenic inflammation. Excitation of both types of nociceptor fibers elicits reflex blinking and irritative tearing.[13,25] In contrast, cold thermoreceptors mediate sensations of ocular surface cooling and drying[22,26] and play an

important role in the modulation of basal tearing and blinking rates associated with the homeostasis of eye surface wetness.[24,27] Surgical injury acutely affects the different classes of sensory axons innervating the ocular surface.[28] However, the degree of residual functional impairment in mechano-nociceptor, polymodal nociceptor, and cold thermoreceptor fibers following PRK, leading eventually to dysesthesias and reflex autonomic disturbances in operated eyes, is still poorly known.

In the present work, we analyzed the changes in spontaneous and stimulus-evoked nerve impulse activity experienced by corneal sensory terminals, immediately and at different times up to 30 days after PRK, while observing the parallel evolution of corneal nerve architecture within and around the wounded area. We discovered that cold-sensitive endings regenerate early albeit a fraction of them, located both in the injured and in the intact peripheral cornea, exhibit an abnormal impulse activity attributable to the incomplete branching of regenerating cold thermoreceptor nerve axons. Polymodal nociceptors and mechano-nociceptors required longer times to recover the normal responsiveness to their natural stimuli.

Methods

Animals

Male, 3- to 6-month-old C57BL/6 mice were purchased from Charles River Laboratory (L'Arbresle Cedex, France). Animals were handled and housed according to the ARVO Statement for the Use of Animals in Ophthalmic and Vision Research and the applicable guidelines of the European Union (2010/63/EU) and the Spanish Government (RD 53/2013). The ethics committee of the University of Oviedo approved all procedures.

Corneal Nerve Injury Through Photorefractive Keratectomy (PRK)

Surgical corneal injury was performed by using a VISX Star S2 excimer laser (VISX, Inc., Santa Clara, CA, USA) as previously described.[29–31] Right eyes were subjected to PRK surgery with the following parameters: a 1.5-mm^2 circular area, 45 μm of depth. The procedure included simultaneous ablation in a single step of the epithelium (using a defined epithelial thickness profile of 25 μm centrally) and 20 μm of the anterior stroma (representing approximately 20% of the total stromal thickness), removing all subbasal nerve fibers and intraepithelial terminals of the treated area.

Before surgery, mice were deeply anesthetized by intraperitoneal injection of a mixture of ketamine hydrochloride (80 mg/kg, Imalgene 1000; Merial Laboratorios S.A., Barcelona, Spain) and xylazine hydrochloride (5 mg/kg, Rompun; Bayer Hispania S.L., Barcelona, Spain) followed by topical application of 0.5% tetracaine chlorhydrate and 1 mg oxybuprocaine (Colircusí Anestésico Doble; Alcon S.A., Barcelona, Spain).

In Vivo Evaluation of Epithelial Wound Healing

Fluorescein staining was used to define the area (mm^2) of the corneal epithelial defect, which was measured under a Leica S6D stereoscopic microscope equipped with an EC3 digital camera (Leica Microsystems, Wetzlar, Germany) and using a fixed magnification of ×12.5. Observations were made immediately after surgery (day 0) and at 3, 7, 15, and 30 days after PRK surgery (T0, T3, T7, T15, and T30, respectively). These time points were selected because they correspond to the moment of important events in the wound-healing process.[29–32] FIJI image analysis software (ImageJ; http://imagej.nih.gov/ij/; provided in the public domain by the National Institutes of Health, Bethesda, MD, USA) was applied to measure the area of fluorescein-impregnated cornea. This was manually lined with the freehand selection tool of FIJI; the software calculated automatically the area inside the selection.

Whole-Mounted Cornea Immunohistochemistry

To obtain the enucleated eyes, animals were deeply anesthetized by intraperitoneal injection with a mixture of ketamine hydrochloride (80 mg/kg) and xylazine hydrochloride (5 mg/kg) and killed by cervical dislocation.

Immunofluorescence

Freshly isolated eyeballs from mice were dissected and fixed 1 hour at room temperature (RT) in methanol and dimethyl sulfoxide (4:1), then were postfixed for 5 minutes in methanol at −21°C. Afterwards, corneas were rehydrated in graded methanol and washed in 0.1 M PBS pH 7.4 (PBS). They were blocked (blocking serum solution) for 1 hour with 5% BSA, 5% goat serum, 0.2% sodium azide, and 0.3% Triton X-100 in PBS (PBS-Triton). After rinsing, corneas were incubated for 24 hours at RT against rabbit anti–neuronal class III β-Tubulin (1:250; Cell Signaling Technology, Boston, MA, USA) in blocking serum solution. After three rinses with 0.2% BSA (washing solution), 0.2% goat serum, 0.2% sodium azide, and PBS-Triton, corneas were incubated in blocking serum solution for 24 hours at RT with secondary antibody against anti-rabbit IgG Alexa Fluor 594 (1:500; Molecular Probes, Eugene, OR, USA). Afterwards, corneas were rinsed three times with washing solution, followed by incubation for 10 minutes at RT with 4′,6-diamidino-2-phenylindole (DAPI, 2 μg/mL; Molecular Probes). Finally, corneas were mounted in slides with fluorescent mounting medium (DAKO, Glostrup, Denmark).

Image Acquisition

Fluorescence images were obtained with a Leica TCS SP8 confocal microscope (Leica Microsystems). For whole-mounted corneas, a mosaic of images was obtained at magnification of ×200 by using tile scan utility of LASX and confocal z stacks, spaced 3.5 μm in the Z-axis.

Morphologic Data Analysis

Images were analyzed by using also the image analysis software FIJI. Whole-mounted corneas were divided in five areas of study (Supplementary Fig. S1): four peripheral zones, which were defined each as two 0.25 mm^2 square regions (a 500 × 500-μm box) whose peripheral borders were approximately 200 μm away from the limbus border and were separated approximately 500 μm from each other; and a fifth area, defined as the injured area in the center of the cornea, which was determined by the absence of DAPI staining in injured corneas (mean injured area, 1.46 ± 0.13 mm^2). This circular area was divided in three concentric circles (Supplementary Fig. S1), with the first and biggest circle corresponding to the border of the injury in PRK-ablated corneas. For comparison, in uninjured corneas the central corneal area was also divided into three similar concentric circular areas of 1.5, 1.0, and 0.5 mm^2.

Subbasal nerves were quantified in the periphery by counting the number of nerves intersecting a line drawn inside the square area (parallel to the limbus; see Supplementary Fig. S1). In the central cornea of both injured and control eyes, subbasal nerves were quantified as the number of nerves intersecting the circumferences defining each of the concen-

tric circles (Supplementary Fig. S1). Nerve density was calculated as the mean number of subbasal nerve fibers per mm^2 entering each circle.

Penetration sites of subepithelial bundles through the epithelial basal lamina were counted within the total area of the cornea. The total number of penetration points, that is, the number of points where axon bundles transverse the basal lamina of corneal epithelium, was counted both outside and inside the largest, 1.5-mm^2 circle by using z-stack images of injured and uninjured corneas, and expressed as number of penetrations per mm^2 in the periphery (outside the circle) and central cornea, respectively.

Electrophysiology

For electrophysiological studies, recordings of single corneal nerve terminals in vitro were performed as previously described.[24] In brief, mice were killed by cervical dislocation and eyes were excised and placed in a physiological saline solution similar to tear fluid (in mM: NaCl [128], KCl [5], NaH_2PO_4 [1], $NaHCO_3$ [26], $CaCl_2$ [2.4], $MgCl_2$ [1.3], and glucose [10]) and bubbled with carbogen gas (5% CO_2 and 95% O_2). The eye was then placed in a recording chamber and was continuously superfused with the same physiological saline solution. Temperature during the experiment was controlled with a homemade Peltier device.

Extracellular electrical activity of single sensory nerve endings of the corneal surface was recorded with a borosilicate glass microelectrode with tip diameter of approximately 50 μm that was filled with saline solution. An Ag/AgCl wire located in the bath serves as indifferent electrode. With the aid of a micromanipulator, the recording pipette was placed on the corneal surface with slight suction at different points both in the injured area and in the periphery (mean of 15 seals per cornea, 10 in injured area and 5 in periphery), searching for nerve terminal impulse (NTI) activity. NTIs were amplified with an AC amplifier (Neurolog NL104; Digitimer, Welwyn, UK) and stored at 10 kHz into a computer, using a CED micro 1401 interface and Spike 2 software (both from Cambridge Electronic Design, Cambridge, UK).

Only recordings containing NTIs originating from a well-defined single nerve terminal were analyzed. In these recordings NTIs were clearly distinguished from noise (~10 μV peak-to-peak) and had similar amplitudes and waveforms, indicating that they originated from the same sensory nerve ending. To minimize deterioration of the preparation with time, the total duration of the experiment was limited to a maximum of 120 minutes per eye (30 minutes for preparation; 90 minutes for recording). Percentage of successful attempts refers to the number of seals made on the cornea in which nerve terminal activity was recorded.

Experimental Protocol

The recording pipette was placed at regularly aligned points on the corneal surface, separated by an approximate distance of 0.2 mm. First, one half of the cornea was explored starting in the center and descending to the periphery; then, the eye was rotated and the opposite side of the cornea was explored.[33] After 90 minutes of recording attempts, the eye was fixed and prepared for morphologic studies.

Cold stimulation was performed by decreasing the background temperature of the perfusing solution (from ~34°C to ~14°C or ~5°C, in cold thermoreceptors or polymodal nociceptors and mechano-nociceptors, respectively), generating a cooling ramp at mean cooling rate of 0.6°C·s^{-1}; when the peak temperature of ~14°C or ~5°C was attained, warming was applied at a similar speed to return to the basal temperature. Following a resting period of 120 seconds, mechanical stimulation was performed by moving forward the pipette with a controlled displacement of the micromanipulator. Pressure with the pipette was maintained for 2 seconds. Two minutes later, a heating ramp (from 34°C to ~52°C at 0.5°C·s^{-1}, ~30 seconds' duration) was applied, returning to the initial control value of 34°C when the peak temperature was reached.

Analysis of NTI Activity

Success percentage indicates the percentage of successful attempts at recording a nerve terminal activity in relation to the total number of attempts. Background activity is defined as the mean basal ongoing frequency in impulses per second (imp·s^{-1}) at the basal temperature (33.9°C ± 0.07°C) measured during the 60-second period that preceded the onset of a stimulus.

The following parameters of the NTI activity were analyzed in the different terminal types.

Cold Thermoreceptor Terminals. *Cooling Threshold.* Temperature (°C) during a cooling ramp at which NTI frequency increased to a value that was the mean NTI frequency measured during the 10-second period preceding the onset of a cooling ramp plus three times its standard deviation.

Cooling Response. Expressed as the mean in NTI frequency between the cooling threshold and the peak response frequency values during the cooling ramp.

Polymodal and Mechano-nociceptor Terminals. *Response to Cooling.* The total number of spikes during the 45 seconds following the onset of the cooling ramp was compared with the total number of spikes during 45 seconds immediately before the cooling ramp.

Response to Heating. The total number of spikes during the 30 seconds following the onset of the heating ramp was compared with the total number of spikes during 30 seconds immediately before the heating ramp.

Response to Mechanical Force. The total number of NTIs during the 10 seconds following the onset of mechanical stimulation was compared with the total number of NTIs during the 10-second period immediately before applying the mechanical stimulus.

Statistical Analysis

Statistical comparisons were performed by using Microsoft Excel 2010 (Microsoft Corporation, Redmond, CA, USA), Origin 8 (OriginLab Corporation, Northampton, MA, USA), and InStat 3 (GraphPad Software, Inc., La Jolla, CA, USA). Data are expressed as mean ± SD. For electrophysiology data unpaired Student's *t*-test was used. The morphologic measurements were compared by using 1-way ANOVA with Tukey-Kramer multiple comparisons post hoc test. Significance threshold was set at $P < 0.05$.

Results

Sixty-five mice were used in this study. PRK was performed in a total of 54 mice. Immediately after laser ablation, fluorescein staining in seven mice delimited in the cornea a circular area of epithelial damage of 2.2 ± 0.1 mm^2. Twenty-four hours later, the size of the injured area in the same animals had decreased to 0.46 ± 0.22 mm^2. The injury was not visible after 2 days in four of the seven mice and was very small in the remaining three (0.05 ± 0.08 mm^2). On the third day, no fluorescein staining was apparent in any of the eyes. PRK caused initially a

marked opacity that reversed progressively with time. Still, 28% of the corneas continued to show light opacity spots 30 days after surgery.

From the 54 operated animals, 26 corneas (at T0, $n = 5$; T3, $n = 4$; T7, $n = 6$; T15, $n = 5$; T30, $n = 6$) and six corneas of intact mice were studied morphologically (Fig. 1A). Electrophysiological recordings were performed in 43 eyes at various times after PRK (T0, $n = 5$; T3, $n = 5$; T7, $n = 15$; T15, $n = 10$; T30, $n = 8$) and in five control eyes where the cornea was intact. The corneas of 15 eyes previously used for electrophysiological recordings were also studied morphologically. In total, electrical activity was recorded from 117 corneal nerve terminals: 66 with receptive fields located within the central area, in the region where the wound was performed, and 51 terminals located in the surrounding peripheral area.

In all recording experiments, the search for nerve terminal impulse activity started by placing the recording electrode on the corneal surface at different pre-established points defined both in the central area where the injury was made and in the intact periphery. From previous studies in intact mice corneas,[33] we defined the fraction of the nerve terminals of the intact cornea responding only to mechanical force as mechano-nociceptors and those activated by heat and mechanical force as polymodal nociceptors. Finally, cold thermoreceptors, initially defined by their responsiveness to cooling, were subclassified by the value of their spontaneous firing at 34°C and the temperature threshold required to increase their firing rate with a cooling ramp[33] as high-background ($\geq$1.5 NTI·s^{-1}), low-threshold ($\geq$30.5°C) cold thermoreceptors (HB-LT), or low-background ($<$1.5 NTI·s^{-1}) high-threshold ($<$30.5°C) cold thermoreceptors (LB-HT). Altogether, in the central cornea 54.1% of the terminals were identified as cold thermoreceptors, 26.7% as polymodal nociceptors, and 10% as mechano-nociceptors. In the peripheral area, 46.7% were cold thermoreceptors; 26.7%, polymodal nociceptors; and 10%, mechano-nociceptors. The remaining units recorded at the central and peripheral cornea could not be accurately classified.

Nerve Terminal Impulse Activity Was Absent From the PRK-Injured Area at Early Stages of Corneal Nerve Regeneration

At day 0, immediately after laser ablation, the corneal epithelium had disappeared and the normal innervation of the central cornea was virtually absent. Only midstromal nerve trunks, often terminating abruptly, could be identified in the stroma, while subepithelial and subbasal plexuses were lost (Figs. 1B, 2B, 3A), and no nerve penetration points were identified in the wounded area (Table). In accordance with this morphologic observation, electrical activity was undetectable within the lesioned area in the animals studied immediately after PRK (Fig. 3A).

In the peripheral cornea surrounding the wounded area, the density of nerve fibers measured after surgery and the number of nerve penetration points in the basal lamina per mm^2 was slightly lower in day 0 corneas than in the same area of the corneas of control mice (Fig. 3B; Table). At this time, the incidence of NTI activity in the peripheral area surrounding the wound was similar in operated and intact corneas (32.4% $\pm$ 9.3%, $n = 5$ at T0 versus 39.1% $\pm$ 7.7%, $n = 5$ in intact corneas; Fig. 3B).

At day 3, regenerating individual rectilinear axons, sprouting from some of the cut subbasal nerves, started to enter the injured region (Figs. 1C, 2C), although most appeared abruptly interrupted at the wound border. The overall density of these regenerating fibers within the damaged area was only 14.3% $\pm$ 3.6% of the density values at the central cornea of intact mice ($P < 0.001$; Fig. 3A, Table). At this time, NTI activity was still undetectable in the wounded area (Fig. 3A).

In the peripheral cornea surrounding the wound, the density of nerve fibers at T3 was significantly lower than in control corneas (Fig. 3B; Table). Likewise, the probability of finding an active nerve terminal at day 3 in the noninjured peripheral cornea was also lower (13.9% $\pm$ 7.9%, $n = 5$; Fig. 3B). Moreover, cold thermosensory terminals exhibiting abnormal low background activity combined with a low cooling threshold, never observed in uninjured corneas, were recorded at the periphery for the first time (Fig. 4).

At day 7 an incipient process of remodeling of the stromal nerves below the wounded area was evident, leading to new basal lamina nerve penetration points that reached near-normal numbers (Table). Entering subepithelial axons were short, tortuous, and ramified (Figs. 1D, 2D). However, at T7 most of the axons present in the ablated area originated from peripheral stumps of subbasal leashes that were growing centrally, but the nerve density remained significantly lower ($P < 0.001$) than in control mice, with nerve density values 51.7% $\pm$ 4.9% of control values (Table). The first nerve terminal electrical activity within the injured corneal area was recorded at this time point and only in 7 of the 13 explored corneas, with the probability of finding an active unit being significantly lower than for the control value (Fig. 3A). Ten active terminals were clearly identified as cold-sensitive. One active terminal with low background activity (0.03 imp·s^{-1}) responded only to mechanical stimulus (from 0 imp/10 s to 71 imp/10 s). In addition, there were three sites with low-amplitude NTIs that could not be identified functionally.

In the peripheral cornea, the mean nerve density increased slightly at T7. In addition, the percentage of points where NTI activity was recorded over the total number of attempts increased to 23.1% $\pm$ 6.5% (Fig. 3B). Six of ten terminals were classified as cold thermoreceptors, while the rest were low-amplitude, functionally unidentifiable terminals.

One Month After PRK, a Subset of the Corneal Endings Exhibited Abnormal Activity Despite the Apparent Morphologic Recovery of the Innervation

At day 15 after injury, the overall density of nerve fibers in the injured area became greater than in the periphery (Table). This was due to a higher number of stromal nerve penetrations (Table) and the incorporation of nerve fibers spreading from the periphery of the wound, forming tortuous and ramified arborizations (Figs. 1E, 2E), although nerve density was still lower (58.9% $\pm$ 3.2%, $P < 0.05$) than in control eyes. At this time, active terminals were found in 6 of 10 corneas, with a higher probability of finding active recording points than at T7 (Fig. 3A). Six of the identified terminals were characterized as cold-sensitive and one as a mechano-nociceptor. In six instances, units with spontaneous activity were observed that had a low amplitude, which decreased further with cooling, preventing reliable identification of their function.

In the peripheral cornea, nerve density continued to increase at T15 in comparison with earlier stages of the study, and the probability of finding NTIs also increased (Fig. 3B; Table), reaching values near those in the periphery of intact corneas. Four active terminals responded clearly to cold stimuli, while four others presented a low amplitude that prevented a reliable functional identification. Another terminal showed the characteristics of a mechanoreceptor (background activity of 0.05 imp·s^{-1}, and 0 imp/10 s before and 14 imp/10 s after mechanical stimulation). One polymodal nociceptor

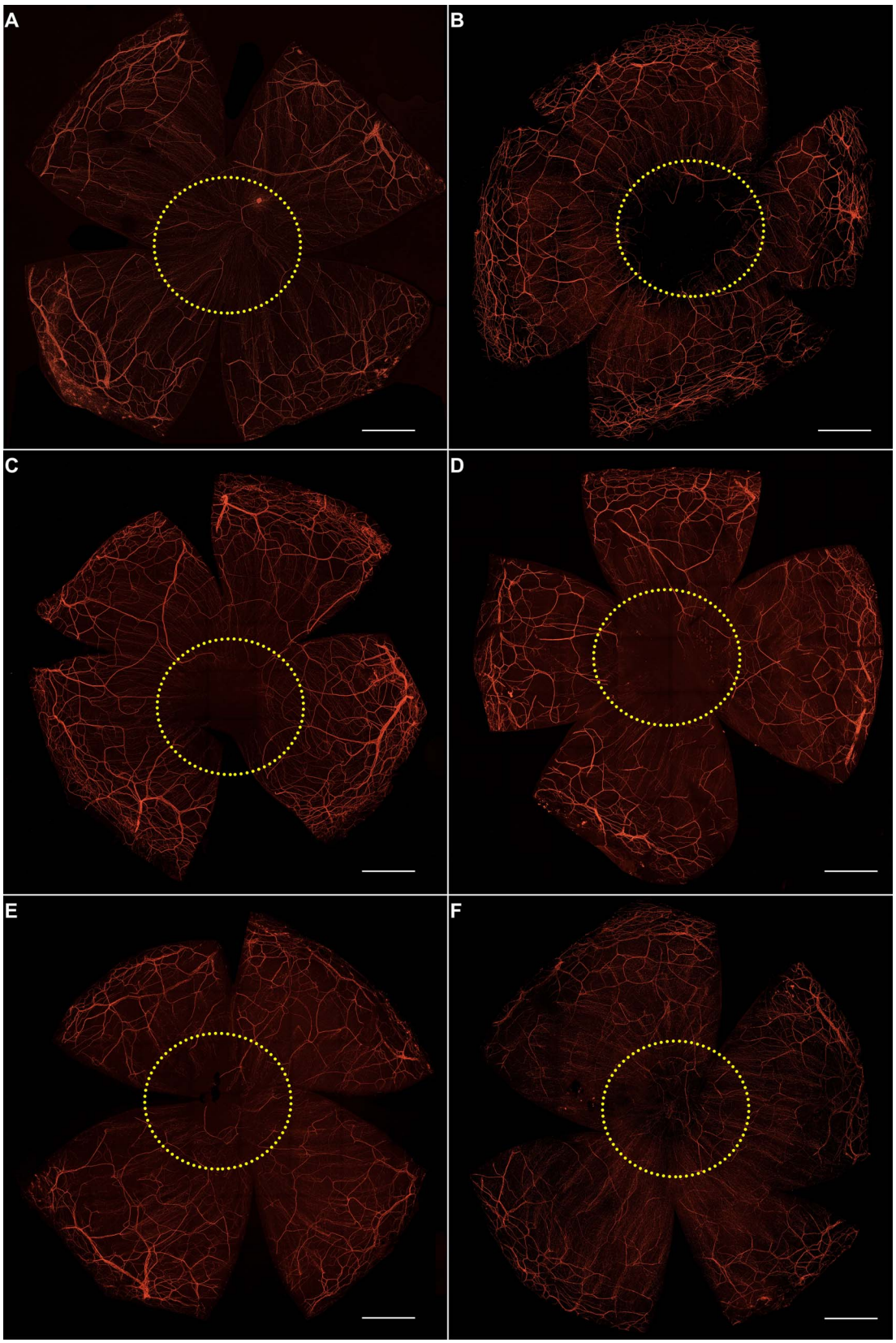

FIGURE 1. Subbasal and stromal corneal nerves at different times after PRK. Whole-mount corneas showing at low magnification (×200) the entire corneal innervation by stromal and subbasal corneal nerves, stained against β-Tubulin III (*red*). (**A**) An intact cornea with the area in which the PRK wound is performed has been marked with a *circle*. (**B**–**F**) Corneas excised and stained at different times after PRK (T0, T3, T7, T15, and T30, respectively). The *circle* indicates in each case the extension of the initial PRK-injured area. *Scale bars*: 500 μm.

Investigative Ophthalmology & Visual Science

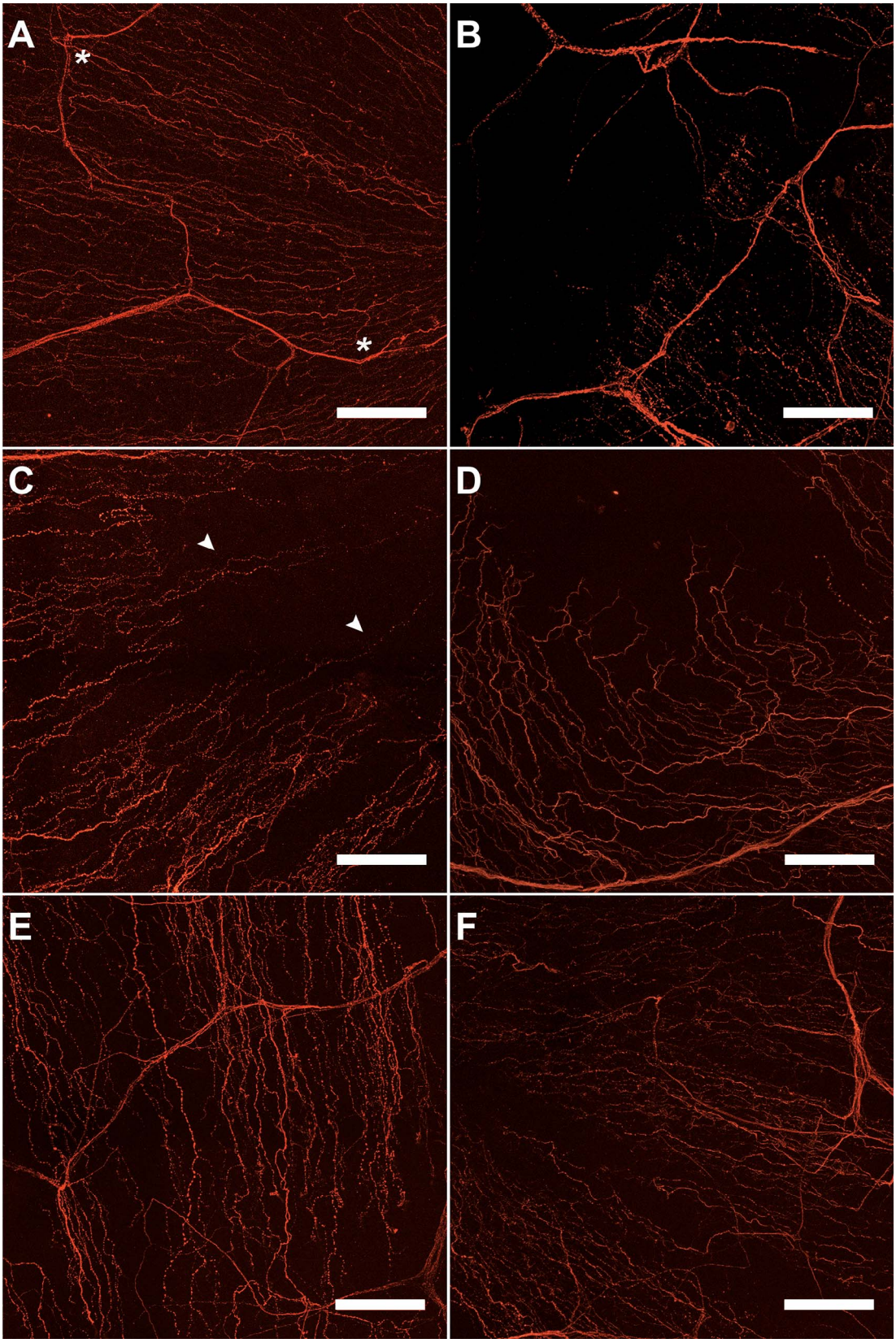

FIGURE 2. Subbasal and stromal corneal nerves at different times after PRK. z-stack images of whole-mount corneas stained against β-Tubulin III (*red*). Images from an intact cornea (**A**) and PRK-operated corneas at different times after PRK ([**B–F**]: T0, T3, T7, T15, and T30, respectively) are shown. *Asterisks* mark the penetration points. No subbasal nerves were observed immediately after PRK (**B**). Three days after ablation, some sprouting subbasal nerves started entering the injured area (*arrowheads*, [**C**]). *Scale bars*: 100 μm.

Investigative Ophthalmology & Visual Science

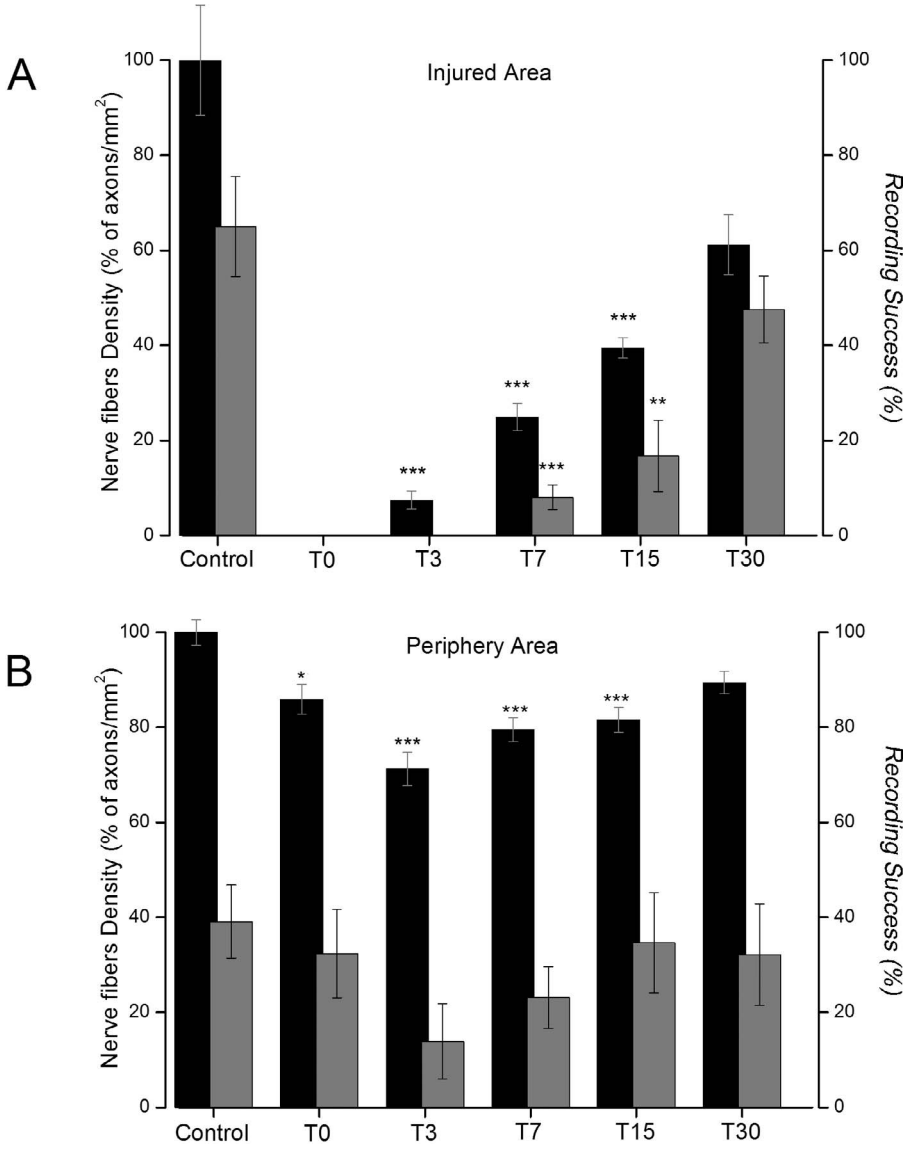

Figure 3. Density of subbasal nerve fibers (*left axis*, *black bars*) and percentage of successful attempts at recording a terminal (*right axis*, *gray bars*) in control eyes and at the different time points after PRK, in the injured area (**A**) and the peripheral, uninjured area (**B**). Nerve density is expressed as percentage of the mean number of axons/mm^2 measured in control corneas in the central (**A**) or the peripheral (**B**) cornea. Successful recording is expressed as percentage of electrophysiological recording attempts where an active corneal unit is found. Statistical analysis compared differences with control group values: $^{*}P$ value < 0.05, $^{**}P$ value < 0.01, $^{***}P$ value < 0.001.

Table. Subbasal Nerve and Epithelial Penetration Point Density Values in the Injured and Peripheral Areas at Different Time Points Post PRK and in Intact Corneas (Control)

	Nerve Density, Axons/mm^2		Penetration Point Density, Points/mm^2	
Experimental Groups	**Injured Area**	**Periphery Area**	**Injured Area**	**Periphery Area**
Control, $n = 6$	574.5 ± 66.5	233.1 ± 6.3	9.9 ± 1.0	8.4 ± 0.4
T0, $n = 5$	0.0 ± 0.0*	200.0 ± 7.2†	0.0 ± 0.0*	8.1 ± 0.4
T3, $n = 4$	42.9 ± 11.0*	166.1 ± 8.2*	0.8 ± 0.5†	7.3 ± 0.3‡
T7, $n = 6$	143.0 ± 16.3*	185.4 ± 5.9*	7.9 ± 1.5	7.1 ± 0.6
T15, $n = 5$	266.5 ± 12.5*	190.0 ± 6.2*	10.0 ± 0.9	8.1 ± 0.4
T30, $n = 6$	351.6 ± 36.1‡	208.5 ± 5.4	9.4 ± 0.4	9.0 ± 0.4

Corneas were processed at 0, 3, 7, 15, and 30 days after surgery (T0, T3, T7, T15, and T30, respectively).
* P value < 0.001.
† P value < 0.05.
‡ P value < 0.01.

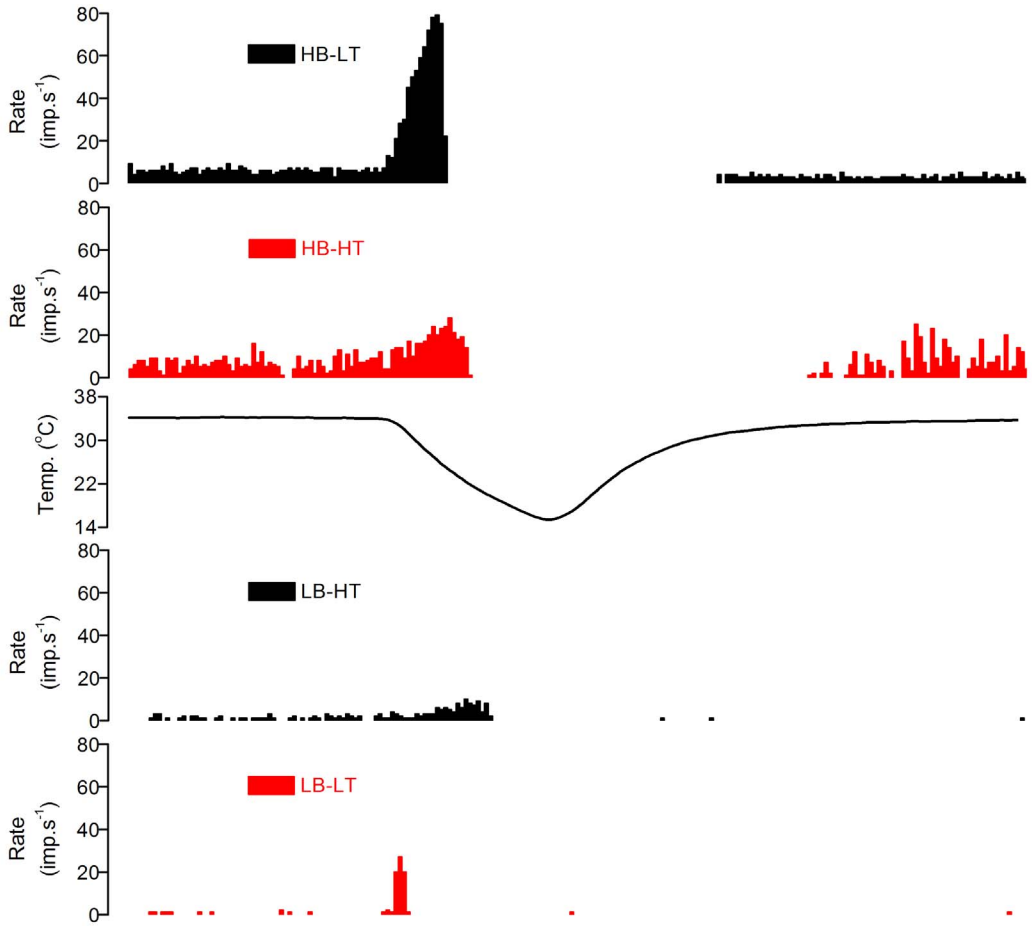

FIGURE 4. Examples of the NTI firing rate recorded in the different subclasses of cold thermoreceptor terminals at 34°C and during application of a cooling ramp down to 15°C. Traces of HB-LT and LB-HT terminals were obtained from control, uninjured mice corneas. Sample recordings of terminals exhibiting abnormal properties (high-background, high-threshold [HB-HT] and low-background, low-threshold [LB-LT] terminals, represented in *red*) were obtained from 30 days post PRK-operated corneas. Middle trace represents the perfusion solution temperature, in °C.

terminal that responded to mechanical stimulation and heat was also found.

At day 30, the overall density of subbasal nerve fibers in the injured area remained significantly lower (75.7% ± 4.1% of control corneas, $P < 0.05$) than in the central region of intact corneas (Figs. 1F, 2F, 3A; Table). Most of the nerve fibers started to organize, forming a vortex in the apex of the cornea. Nonetheless, a low number of axons still showed an erratic distribution. For the first time in the study, NTI activity was present in the injured area of all corneas tested ($n = 8$). The probability that the recording at defined points contained an active terminal was 47.5% ± 7% ($n = 8$), still below the values found in the central cornea of control eyes (65% ± 10.5%, $n = 5$) (Fig. 3A). Of the 27 active terminals found in operated corneas at T30, 5 were defined as polymodal nociceptors and 7 as cold thermoreceptors. At the remaining 15 recording sites the NTIs had a low amplitude and could not be accurately categorized.

In the corneal periphery surrounding the wounded area, the mean nerve density at T30 was similar to the same area in the intact corneas. At this time the probability of finding sites with nerve activity was 32.1% ± 10.1% (Fig. 3B; Table). Of the eight units recorded, two were characterized as cold thermoreceptors, one as polymodal, and one as a mechano-nociceptor. The remaining four units had low-amplitude NTIs, preventing reliable functional identification.

A Fraction of Cold Thermoreceptor Endings Remain Functionally Altered 30 Days After PRK

Collectively, at all times after injury, the firing of high-background cold thermoreceptor terminals found in the injured area was abnormal. HB-LT cold thermoreceptor terminals found in the injured area had on the average lower background activity and cooling response values than those of the same area seen in the healthy cornea (background activity: 3.4 ± 0.5 versus 6.1 ± 0.7 imp·s^{-1}, $P < 0.05$; cooling response: 21.5 ± 4.2 versus 34.2 ± 2.3 imp·s^{-1}, $P < 0.01$; injured, $n = 20$ versus healthy, $n = 10$). LB-HT terminals also responded less to cooling (3.3 ± 0.9 versus 6.1 ± 0.7 imp·s^{-1}, $P < 0.05$; injured, $n = 6$ versus healthy, $n = 6$). Moreover, in the injured and also in the surrounding undamaged area, we frequently observed terminals exhibiting low background activity (<1.5 imp·s^{-1} at 34°C), but combined with an abnormally low cold threshold (LB-LT). These units were observed first in the uninjured area at T3 and in the injured and uninjured area since T7. Conversely, other terminals had a high background frequency at 34°C (>1.5 imp·s^{-1}) but a cooling threshold below 30.5°C (HB-HT). Figure 4 shows an example of the firing pattern of these abnormal cold thermoreceptor terminal types. The overall incidence of abnormal units decreased during the healing period, from 37.5% 1 week after injury to approximately 22.2% 1 month later.

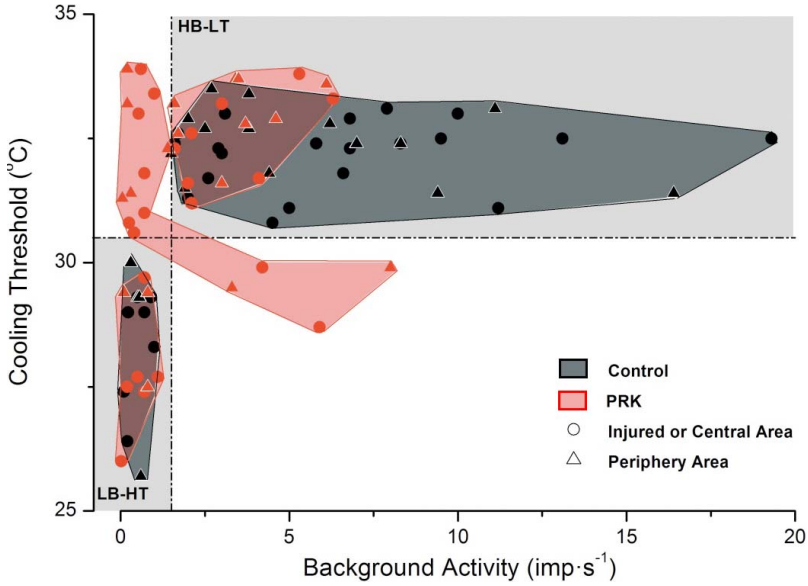

Figure 5. Distribution of corneal cold thermoreceptor terminals attendant on thermal threshold and background firing frequency. Terminals from intact, control corneas are represented with *black symbols* (*circles*, central area; *triangles*, peripheral area). Terminals recorded in PRK-operated corneas (3–30 days after surgery) are represented with *red symbols* (*circles*, terminals in the central, injured area; *triangles*, terminals of the uninjured periphery). The *horizontal* and *vertical interrupted lines* delimit respectively the values of threshold and background activity used to define terminals as HB-LT and LB-HT cold thermoreceptor types (*gray quadrants*). Some terminals of PRK-operated corneas located outside the gray quadrants of the graph possess mixed firing characteristics (high background, high threshold [HB-HT] and low background, low threshold [LB-LT]).

In Figure 5, the whole population of corneal cold thermoreceptor terminals recorded in intact corneas and in injured cornea at all postinjury days is plotted, grouped by their mean background NTI frequency at 34°C and the cooling threshold during a cooling ramp. This representation segregates clearly the canonical HB-LT thermoreceptor terminals from the LB-HT thermoreceptors, the two functional types found in intact corneas (Figs. 4, 5, shown in black). This representation also highlights the presence in PRK-treated corneas of a fraction of terminals (red symbols) that maintain the firing characteristics of typical HB-LT and LB-HT cold thermoreceptor terminals, although as indicated earlier, they present on average lower values of background activity than those of intact corneas. Figure 5 also delimits the well-defined population of abnormal cold-sensitive terminals, displaying mixed firing characteristics found in the injured and the intact area of PRK-treated corneas.

Activity of Polymodal Nociceptors in the Injured Area Reappears Only 30 Days After PRK

Endings with low background activity or silent at rest but activated by heat and mechanical stimulation were absent in the recordings performed in the injured cornea until T30. In eight corneas studied at this time, 5 of the 27 active terminals were classified as polymodal nociceptors. They presented a low background activity of 0.5 ± 0.2 imp·s^{-1} ($n = 5$). As occurs with polymodal nociceptors of the intact cornea, this background activity decreased during a cooling ramp so that the total number of impulses fired during the 45-second period before cooling (mean, 25 ± 11.8 NTIs; $n = 5$) decreased during the 45-second cooling ramp to 16.4 ± 5.4 NTIs ($n = 5$). Conversely, polymodal terminals responded clearly to heating (7.3 ± 1.9 imp/30 s before and 37.8 ± 10.7 imp/30 s during a heating ramp, $n = 5$) and clearly increased their firing rate in response to mechanical stimulation (2.8 ± 0.4 NTIs/10 s before and 22 ± 13.8 imp/10 s during mechanical stimulation).

In the periphery, polymodal nociceptor activity was also practically absent until T7, with only one terminal responding to heat and to mechanical stimulation at T3. Terminals presenting the characteristics of polymodal nociceptors were identified at T15 and T30; altogether, their incidence was lower, around 10% in lesioned versus 27% in intact corneas.

Discussion

The present work confirms the occurrence of extensive morphologic and functional damage to corneal nerves after application of the photoablation procedure used in refractive surgery, and uncovers the marked differences in time course required by corneal sensory nerve fibers of different modality (polymodal nociceptors, mechano-nociceptors, and cold thermoreceptors) to regenerate, and to recover, albeit partially, their normal responsiveness to natural stimuli. Our study additionally revealed that the functional disturbances caused by injury affect also nerve terminals outside the directly wounded area, especially in cold thermoreceptors, possibly reflecting damage by PRK to some terminal branches of parent axons that entered the wound area but that predominantly had their sensory nerve terminals in the noninjured parts of the cornea.

PRK is a procedure that completely removes the epithelium and approximately 20 μm of the anterior stroma of treated corneas, thus affecting the small and medium-sized nerve bundles running in the anterior stromal plexus, particularly its more anterior, dense part, the subepithelial plexus.[34] The laser beam directly destroys the more superficial nerve branches in the treated area, while the distal segments of axons running in a large extent outside the lesion, but affected by the laser beam, degenerate rapidly. Our work confirms previous studies reporting that within hours after PRK, nerves are totally absent from the injured area and those in the surrounding periphery are reduced in number.[16]

In human patients, nerve regeneration is slow. Subbasal nerve fiber bundles visualized with tandem scanning confocal microscopy are present only in 17% of the corneas 1 month after PRK, and the density of these nerve fibers is 98% less than preoperatively. After approximately 3 months, no branched nerve fibers can be seen in the center of the ablation zone; mean subbasal nerve density remains reduced by 59% at 1 year, when compared with preoperative values.[18,35] By 2 years, subbasal nerve density after PRK is similar but morphologic alterations are still present even 5 years after PRK.[36] Despite the timescale differences in regeneration speed between mice and humans, our study showed that recovery of nerve fiber density in the cornea of mice following PRK is also slow, and 1 month later has not fully reestablished the original architecture of corneal innervation.

Maintenance and remodeling of mature axons depend under normal circumstances on extrinsic signals from the environment, which activate their translational machinery, inducing the synthesis of proteins involved in the dynamic regulation of the cytoskeleton.[37] Nerve injury locally generates a cascade of retrograde signaling events that ultimately activate the transcription of genes required for axon survival and regrowth after axotomy.[38–40] Extrinsic signals acting on growth cones of the damaged axons shape the outgrowth pattern regulating the local synthesis of positive and negative regulators of cytoskeletal dynamics, thereby defining the trajectory and length of the growing fibers.[40] In addition to chemotropic cues, mechanical forces exerted by the extruding basal cells during epithelial cell proliferation accompanying corneal wound healing may also influence axonal growth. These forces are transmitted to the subbasal axons and to the reassembling epithelial basement membrane, likely affecting adhesion between epithelial cells, basement membrane, and subbasal axons and thereby, the navigation of regenerating axons.[41] Considering the numerous positive and negative regulators influencing the final trajectory and elongation of axons after injury, the slow and incomplete recovery of the prelesion innervation architecture after PRK is not surprising.[42]

Our study revealed that the appearance of sprouting axons within the injured area does not imply an immediate and parallel recovery of their function. In fact, we observed that corneal sensory terminals of different modality required variable times to recuperate responsiveness to their natural stimuli. Cold thermoreceptor terminals began to respond 1 week after surgery as occurs with mechano-nociceptors, while the first recordings of identifiable polymodal units in the injured area were obtained only 3 weeks later. It is well established that sensory ganglion neurons underlying the various somatosensory modalities possess different genetic signatures, immunocytochemical characteristics, and functional properties.[43,44] The longer time required by polymodal nociceptor neurons to restore their peripheral membrane excitability and transduction properties after PRK may reflect a distinct responsiveness of these nociceptors to the injury-triggered molecular signals responsible for rebuilding the ionic mechanisms required for the transduction and coding of specific stimuli during the regeneration process.[45] Moreover, corneal polymodal nociceptor axons are sparsely branched, generally with simple or ramifying epithelial endings.[46,47] It is therefore possible that in most cases destruction of polymodal axons by PRK affects most if not all the branches of a parent axon within the epithelium and subepithelium, thus requiring a longer time to regenerate. In contrast, cold thermoreceptor corneal axons branch very extensively and form predominantly complex endings,[24,47] a part of which may be spared from injury, thus facilitating regeneration. Still, 30 days after PRK, NTI activity of cold thermoreceptor endings within the treated area is often abnormal, suggesting that the recovery of electrophysiological properties at this time is still incomplete.

Background firing rate and dynamic sensitivity to cold of intact cold thermoreceptors depend on the level of expression of cold-activated TRPM8 channels and the modulation of their terminals' excitability by Kv and HCN channels.[48–50] It has been postulated that action potential firing of cold thermoreceptors originates within a single spatially restricted region of the nerve terminal arbor of the parent axon, where each separate branch encodes individual action potentials autonomously.[51–53]

Altered architecture of cold terminals and abnormal expression of ion channels involved in cold transduction and coding after injury likely decrease both the transducing membrane surface and the number of membrane points at which propagated impulses may generate. Both circumstances are expected to contribute to the lower background frequency and abnormal firing observed in cold thermoreceptor terminals of the injured cornea after PRK.

Notably, abnormal background activity and altered cooling responses were also observed in some of the cold thermoreceptor endings recorded into the intact cornea surrounding the PRK wound. We hypothesize that these terminals belong to cold thermoreceptor parent axons that had originally some branches extending into the operated area. Their loss after PRK reduced the total number of branches at which NTIs originate, thereby decreasing background frequency and responsiveness to cold. The same abnormal firing has been reported in cold thermoreceptor axons of very old mice, where axonal terminal branching is drastically reduced.[54]

Tearing disturbances and dryness sensation in humans appear often after PRK.[1,2] Acute, strong pain usually disappears a few days after surgery, coincident with corneal re-epithelization, which protects the intact and injured terminals against direct exposure to environmental challenges. However, sensations described as "sharp pains," "eyelid sticking to the eyeball," or "soreness of the eyelid to touch" occur 6 or more months after surgery in 5% to 25% of patients, while nearly 50% report feelings of "dryness."[55] Corneal cold thermoreceptor fibers are implicated in the regulation of basal tearing rate and have been proposed also as the source of the unpleasant dryness sensation associated with dry eye disease.[13,20,24,26] The differences in time course and characteristics of disturbances in corneal nerve activity observed in mice after PRK confirm the important role played by aberrant impulse activity in axotomized nerves for the appearance of dysesthesias following PRK[56] and lend support to the proposal that, among the different functional subclasses of corneal nerves, cold thermoreceptors are major players in the development of phantom unpleasant dryness sensation after photorefractive surgery procedures.

Acknowledgments

The authors thank the contribution of Rodolfo Madrid and James A. Brock for critical reading of the manuscript.

Supported by FC-15-GRUPIN14-141 (Consejería de Economía y Empleo, Asturias, Spain); SAF2014-54518-C3-1-R, SAF2014-54518-C3-2-R, SAF2017-83674-C2-1-R, and SAF2017-83674-C2-2-R (Ministerio de Economía, Industria y Competitividad, Spain, and European Regional Development Funds, European Union), and the Spanish "Severo Ochoa" Program for Centers of Excellence in R&D (SEV-2013-0317). Funding from Fundación Ramón Areces and Caja Rural de Asturias, Spain, and European Commission H2020 GA No. 667400 are also acknowledged.

Disclosure: **F. Bech**, None; **O. González-González**, None; **E. Artime**, None; **J. Serrano**, None; **I. Alcalde**, None; **J. Gallar**, None; **J. Merayo-Lloves**, None; **C. Belmonte**, None

References

1. Tuunanen TH, Tervo TM. Schirmer test values and the outcome of photorefractive keratectomy. *J Cataract Refract Surg*. 1996;22:702–708.
2. Ang RT, Dartt DA, Tsubota K. Dry eye after refractive surgery. *Curr Opin Ophthalmol*. 2001;12:318–322.
3. Nejima R, Miyata K, Tanabe T, et al. Corneal barrier function, tear film stability, and corneal sensation after photorefractive keratectomy and laser in situ keratomileusis. *Am J Ophthalmol*. 2005;139:64–71.
4. Kymionis GD, Tsiklis NS, Ginis H, Diakonis VF, Pallikaris I. Dry eye after photorefractive keratectomy with adjuvant mitomycin C. *J Refract Surg*. 2006;22:511–513.
5. Okamoto K, Tashiro A, Thompson R, Nishida Y, Bereiter DA. Trigeminal interpolaris/caudalis transition neurons mediate reflex lacrimation evoked by bright light in the rat. *Eur J Neurosci*. 2012;36:3492–3499.
6. Katagiri A, Thompson R, Rahman M, Okamoto K, Bereiter DA. Evidence for TRPA1 involvement in central neural mechanisms in a rat model of dry eye. *Neuroscience*. 2015;290:204–213.
7. Gallar J, Acosta MC, Moilanen JA, Holopainen JM, Belmonte C, Tervo TM. Recovery of corneal sensitivity to mechanical and chemical stimulation after laser in situ keratomileusis. *J Refract Surg*. 2004;20:229–235.
8. Nettune GR, Pflugfelder SC. Post-LASIK tear dysfunction and dysesthesia. *Ocul Surf*. 2010;8:135–145.
9. Ambrosio R Jr, Tervo T, Wilson SE. LASIK-associated dry eye and neurotrophic epitheliopathy: pathophysiology and strategies for prevention and treatment. *J Refract Surg*. 2008;24:396–407.
10. Kaminer J, Powers AS, Horn KG, Hui C, Evinger C. Characterizing the spontaneous blink generator: an animal model. *J Neurosci*. 2011;31:11256–11267.
11. Gartry DS, Muir MG, Lohmann CP, Marshall J. The effect of topical corticosteroids on refractive outcome and corneal haze after photorefractive keratectomy: a prospective, randomized, double-blind trial. *Arch Ophthalmol*. 1992;110:944–952.
12. Kirveskari J, Helinto M, Saaren-Seppala H, Renkonen R, Tervo T. Leukocyte rolling and extravasation in surgical inflammation after mechanical and laser-induced trauma in human patients. *Exp Eye Res*. 2003;77:387–390.
13. Belmonte C, Acosta MC, Merayo-Lloves J, Gallar J. What causes eye pain? *Curr Ophthalmol Rep*. 2015;3:111–121.
14. Torricelli AA, Santhanam A, Wu J, Singh V, Wilson SE. The corneal fibrosis response to epithelial-stromal injury. *Exp Eye Res*. 2016;142:110–118.
15. Rozsa AJ, Guss RB, Beuerman RW. Neural remodeling following experimental surgery of the rabbit cornea. *Invest Ophthalmol Vis Sci*. 1983;24:1033–1051.
16. Tervo K, Latvala TM, Tervo TM. Recovery of corneal innervation following photorefractive keratoablation. *Arch Ophthalmol*. 1994;112:1466–1470.
17. Erie JC. Corneal wound healing after photorefractive keratectomy: a 3-year confocal microscopy study. *Trans Am Ophthalmol Soc*. 2003;101:293–333.
18. Erie JC, McLaren JW, Hodge DO, Bourne WM. Recovery of corneal subbasal nerve density after PRK and LASIK. *Am J Ophthalmol*. 2005;140:1059–1064.
19. Belmonte C, Aracil A, Acosta MC, Luna C, Gallar J. Nerves and sensations from the eye surface. *Ocul Surf*. 2004;2:248–253.
20. Belmonte C, Nichols JJ, Cox SM, et al. TFOS DEWS II pain and sensation report. *Ocul Surf*. 2017;15:404–437.
21. Acosta MC, Tan ME, Belmonte C, Gallar J. Sensations evoked by selective mechanical, chemical, and thermal stimulation of the conjunctiva and cornea. *Invest Ophthalmol Vis Sci*. 2001;42:2063–2067.
22. Acosta MC, Belmonte C, Gallar J. Sensory experiences in humans and single-unit activity in cats evoked by polymodal stimulation of the cornea. *J Physiol*. 2001;534:511–525.
23. Acosta MC, Peral A, Luna C, Pintor J, Belmonte C, Gallar J. Tear secretion induced by selective stimulation of corneal and conjunctival sensory nerve fibers. *Invest Ophthalmol Vis Sci*. 2004;45:2333–2336.
24. Parra A, Madrid R, Echevarria D, et al. Ocular surface wetness is regulated by TRPM8-dependent cold thermoreceptors of the cornea. *Nat Med*. 2010;16:1396–1399.
25. Belmonte C, Tervo T, Gallar J. Sensory innervation of the eye. In: Levin L, Nilsson S, Ver Hoeve J, Wu S, Kaufman P, Alm A, eds. *Adler's Physiology of the Eye*. Saunders Elsevier; 2011:363–384.
26. Kovacs I, Luna C, Quirce S, et al. Abnormal activity of corneal cold thermoreceptors underlies the unpleasant sensations in dry eye disease. *Pain*. 2016;157:399–417.
27. Quallo T, Vastani N, Horridge E, et al. TRPM8 is a neuronal osmosensor that regulates eye blinking in mice. *Nat Commun*. 2015;6:7150.
28. Gallar J, Acosta MC, Gutierrez AR, Belmonte C. Impulse activity in corneal sensory nerve fibers after photorefractive keratectomy. *Invest Ophthalmol Vis Sci*. 2007;48:4033–4037.
29. Anitua E, Sanchez M, Merayo-Lloves J, De la Fuente M, Muruzabal F, Orive G. Plasma rich in growth factors (PRGF-Endoret) stimulates proliferation and migration of primary keratocytes and conjunctival fibroblasts and inhibits and reverts TGF-beta1-induced myodifferentiation. *Invest Ophthalmol Vis Sci*. 2011;52:6066–6073.
30. Alcalde I, Inigo-Portugues A, Carreno N, Riestra AC, Merayo-Lloves JM. Effects of new biomimetic regenerating agents on corneal wound healing in an experimental model of post-surgical corneal ulcers. *Arch Soc Esp Oftalmol*. 2015;90:467–474.
31. Reimondez-Troitino S, Alcalde I, Csaba N, et al. Polymeric nanocapsules: a potential new therapy for corneal wound healing. *Drug Deliv Transl Res*. 2016;6:708–721.
32. Martinez-Garcia MC, Merayo-Lloves J, Blanco-Mezquita T, Mar-Sardana S. Wound healing following refractive surgery in hens. *Exp Eye Res*. 2006;83:728–735.
33. Gonzalez-Gonzalez O, Bech F, Gallar J, Merayo-Lloves J, Belmonte C. Functional properties of sensory nerve terminals of the mouse cornea. *Invest Ophthalmol Vis Sci*. 2017;58:404–415.
34. Marfurt CF, Cox J, Deek S, Dvorscak L. Anatomy of the human corneal innervation. *Exp Eye Res*. 2010;90:478–492.
35. Erie EA, McLaren JW, Kittleson KM, Patel SV, Erie JC, Bourne WM. Corneal subbasal nerve density: a comparison of two confocal microscopes. *Eye Contact Lens*. 2008;34:322–325.
36. Moilanen JA, Vesaluoma MH, Müller LJ, Tervo TM. Long-term corneal morphology after PRK by in vivo confocal microscopy. *Invest Ophthalmol Vis Sci*. 2003;44:1064–1069.
37. Michaelevski I, Segal-Ruder Y, Rozenbaum M, et al. Signaling to transcription networks in the neuronal retrograde injury response. *Sci Signal*. 2010;3:ra53.
38. Vogelaar CF, Gervasi NM, Gumy LF, et al. Axonal mRNAs: characterisation and role in the growth and regeneration of dorsal root ganglion axons and growth cones. *Mol Cell Neurosci*. 2009;42:102–115.
39. Gumy LF, Tan CL, Fawcett JW. The role of local protein synthesis and degradation in axon regeneration. *Exp Neurol*. 2010;223:28–37.
40. Jung H, Yoon BC, Holt CE. Axonal mRNA localization and local protein synthesis in nervous system assembly, maintenance and repair. *Nat Rev Neurosci*. 2012;13:308–324.

41. Pal-Ghosh S, Pajoohesh-Ganji A, Tadvalkar G, et al. Topical Mitomycin-C enhances subbasal nerve regeneration and reduces erosion frequency in the debridement wounded mouse cornea. *Exp Eye Res*. 2016;146:361–369.
42. Namavari A, Chaudhary S, Sarkar J, et al. In vivo serial imaging of regenerating corneal nerves after surgical transection in transgenic thy1-YFP mice. *Invest Ophthalmol Vis Sci*. 2011; 52:8025–8032.
43. Lallemend F, Ernfors P. Molecular interactions underlying the specification of sensory neurons. *Trends Neurosci*. 2012;35: 373–381.
44. Usoskin D, Furlan A, Islam S, et al. Unbiased classification of sensory neuron types by large-scale single-cell RNA sequencing. *Nat Neurosci*. 2015;18:145–153.
45. Hu G, Huang K, Hu Y, et al. Single-cell RNA-seq reveals distinct injury responses in different types of DRG sensory neurons. *J Neurosci*. 2016;6:31851.
46. Alamri A, Bron R, Brock JA, Ivanusic JJ. Transient receptor potential cation channel subfamily V member 1 expressing corneal sensory neurons can be subdivided into at least three subpopulations. *Front Neuroanat*. 2015;9:71.
47. Ivanusic JJ, Wood RJ, Brock JA. Sensory and sympathetic innervation of the mouse and guinea pig corneal epithelium. *J Comp Neurol*. 2013;521:877–893.
48. Viana F, de la Pena E, Belmonte C. Specificity of cold thermotransduction is determined by differential ionic channel expression. *Nat Neurosci*. 2002;5:254–260.
49. Madrid R, de la Peña E, Donovan-Rodriguez T, Belmonte C, Viana F. Variable threshold of trigeminal cold-thermosensitive neurons is determined by a balance between TRPM8 and Kv1 potassium channels. *J Neurosci*. 2009;29:3120–3131.
50. Orio P, Parra A, Madrid R, Gonzalez O, Belmonte C, Viana F. Role of Ih in the firing pattern of mammalian cold thermoreceptor endings. *J Neurophysiol*. 2012;108:3009–3023.
51. Brock JA, Pianova S, Belmonte C. Differences between nerve terminal impulses of polymodal nociceptors and cold sensory receptors of the guinea-pig cornea. *J Physiol*. 2001;533:493–501.
52. Carr RW, Pianova S, Fernandez J, Fallon JB, Belmonte C, Brock JA. Effects of heating and cooling on nerve terminal impulses recorded from cold-sensitive receptors in the guinea-pig cornea. *J Gen Physiol*. 2003;121:427–439.
53. Carr RW, Pianova S, McKemy DD, Brock JA. Action potential initiation in the peripheral terminals of cold-sensitive neurones innervating the guinea-pig cornea. *J Physiol*. 2009;587:1249–1264.
54. Alcalde I, Íñigo-Portugués A, González-González O, et al. Morphological and functional changes in TRPM8-expressing corneal cold thermoreceptor neurons during aging and their impact on tearing in mice [published online ahead of print April 17, 2018]. *J Comp Neurol*. doi:10.1002/cne.24454.
55. Hovanesian JA, Shah SS, Maloney RK. Symptoms of dry eye and recurrent erosion syndrome after refractive surgery. *J Cataract Refract Surg*. 2001;27:577–584.
56. Belmonte C. Eye dryness sensations after refractive surgery: impaired tear secretion or "phantom" cornea? *J Refract Surg*. 2007;23:598–602.

Investigative Ophthalmology & Visual Science